

EVOLUTION OF THE FLOW FIELD AROUND A CIRCULAR CYLINDER AND A SPHERE UPON INSTANTANEOUS START WITH A SUPERSONIC VELOCITY

V. A. Bashkin, I. V. Egorov, and D. V. Ivanov

UDC 533.6.011.8

Evolution of the flow field around a circular cylinder and a sphere instantaneously starting with a constant supersonic velocity ($M_\infty = 5$ and $Re = 10^5$) from the state at rest is studied by means of numerical integration of unsteady two-dimensional Navier–Stokes equations.

Key words: *supersonic flow, instantaneous start, cylinder, sphere.*

Introduction. One of the problems of unsteady aerohydrodynamics is starting of a body with a constant velocity from the state at rest.

In an incompressible liquid, small perturbations propagate with an infinite velocity; therefore, an inviscid potential flow with a tangential discontinuity (infinitely thin vortex layer) on the wetted surface is formed near the body in the case of instantaneous start. At later times, diffusion of the vortex layer into the ambient space occurs owing to internal friction forces. If the motion proceeds at a sufficiently high Reynolds number, a viscous flow begins to develop in the boundary layer with a known pressure distribution [1, 2]. Thus, prior to boundary-layer separation ($t < t_s$), the inviscid and viscous flows exist almost independently. At $t \geq t_s$, they start interacting, which leads to significant reconstruction of the flow field around the body considered. This stage of flow evolution is theoretically examined on the basis of Navier–Stokes equations.

In a gas, small perturbations propagate with a finite velocity; hence, the inviscid flow and the boundary-layer flow start to develop almost simultaneously and interact with each other. In this case, the unsteady process at all stages is also considered on the basis of Navier–Stokes equations.

A technique of numerical integration of unsteady two-dimensional Navier–Stokes equations developed in [3, 4] allows numerical simulation of a supersonic flow over plane and axisymmetric bodies. The steady flow regime, if existing under given conditions, is obtained as the limiting case as $t \rightarrow \infty$ (time-dependent method). This technique was tested by solving a number of problems of internal and external aerodynamics. In particular, a supersonic steady flow around a circular cylinder was calculated.

In the present work, we used this technique of numerical simulation to study evolution of the flow field around a circular cylinder and a sphere of radius R in the case of their instantaneous start from the state at rest with a constant supersonic velocity corresponding to the Mach number $M_\infty = 5$. Motion of the bodies proceeds with a Reynolds number $Re = \rho_\infty V_\infty R / \mu_\infty = 10^5$ (V_∞ , ρ_∞ , and μ_∞ are the velocity, density, and dynamic viscosity of the free-stream gas). The surfaces of the bodies were assumed to be isothermal with a temperature T_w ; the temperature factor is $T_w / T^* = 0.5$ (T^* is the free-stream stagnation temperature).

The computations were performed for a symmetric flow on a 201×201 nonuniform grid with a constant time step $\Delta t = 0.01$. The origin of the Cartesian (cylindrical) coordinate system is aligned with the center of the body. The computational domain is asymmetric: its upstream boundary is located at a distance of $5R$, the downstream boundary is located at a distance of $15R$, and the boundary in the normal direction is located at a distance of $11R$.

Flow Field Structure. The basic features of flow field evolution near the cylinder and the sphere are qualitatively identical. At the time $t = 0$, there is a uniform supersonic flow over the bodies considered. At

Zhukovskii Central Aerohydrodynamic Institute, Zhukovskii 140180. Translated from *Prikladnaya Mekhanika i Tekhnicheskaya Fizika*, Vol. 45, No. 3, pp. 44–49, May–June, 2004. Original article submitted January 14, 2003; revision submitted July 14, 2003.

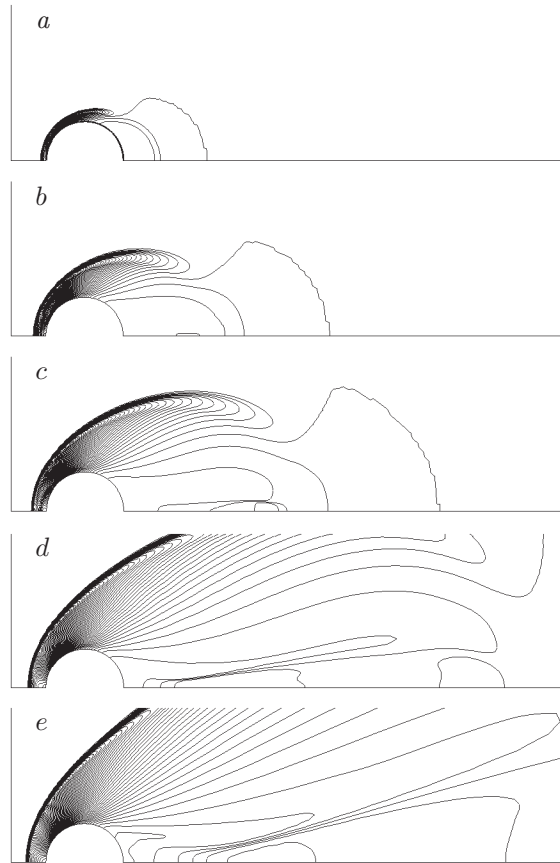


Fig. 1. Isolines $c_p = \text{const}$ around a circular isothermal cylinder ($M_\infty = 5$ and $\text{Re} = 10^5$): $\bar{t} = 1$ (a), 3 (b), 5 (c), 10 (d), and 50 (e).

subsequent times, the flow impinges onto the frontal part of the body, and its interaction with the wetted surface leads to formation of a bow shock wave and a compression region ahead of the body. In the rear part of the body, the flow moves away from the surface and forms a rarefaction wave behind; with time, this wave leaves the computational domain, moving to an infinitely distant point downstream, and the structure of the near and far wake is formed behind the wave.

Figure 1 shows the time evolution of isolines of the pressure coefficient $c_p = (p - p_\infty)/q_\infty$ near the circular cylinder ($q_\infty = 0.5\rho_\infty V_\infty^2$ is the free-stream dynamic pressure). At the initial time, the disturbed flow region is concentrated in the neighborhood of the body. By the time $\bar{t} = t/t_R = 1$ ($t_R = R/V_\infty$), a thin shock layer is formed on the leeward side of the body (Fig. 1a); the shape of its external boundary is close to an arc. A rarefaction region whose downstream size is of the order of the characteristic linear size is formed behind the body. The isobar separating the compression and rarefaction regions starts near the mid-section of the body.

Afterwards, the disturbed flow region increases. At the initial stage, an attached flow is formed, and a global zone of separated flow is formed in the base region in the vicinity of the rear stagnation point at the time $\bar{t} \approx 3$ for a cylinder and $\bar{t} \approx 2$ for a sphere.

The shock wave is formed in the neighborhood of the plane of symmetry of the cylinder (Fig. 1b). Then, the shock wave propagates upstream from the plane of symmetry (Fig. 1c and d) and extends to the entire flow field (Fig. 1e). Simultaneously, the separation region is developed behind the body, and a flow structure typical of a blunted body in a supersonic flow is gradually formed.

Isolines of other gas-dynamic variables allow obtaining additional information. In particular, an analysis of vorticity fields shows that vorticity is generated by two sources. The first source is a curved bow shock wave, where the inviscid mechanism of vorticity generation operates in accordance with the Crocco theorem. Another, more powerful source is the solid wall where the viscous mechanism of vorticity generation operates because no-slip conditions are satisfied there.

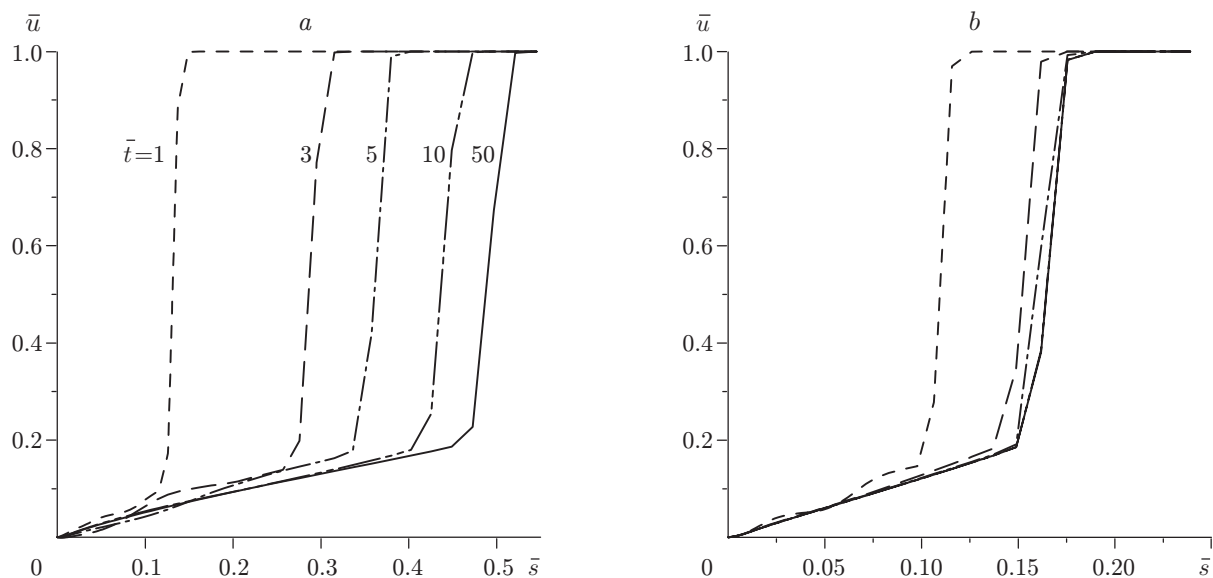


Fig. 2. Distribution of velocity $\bar{u} = u/V_\infty$ on the axis of symmetry ahead of an isothermal cylinder (a) and an isothermal sphere (b) at different times.

Flow on the Plane (Axis) of Symmetry ahead of the Body. Additional information on the specific features of flow evolution ahead of the bodies considered can be obtained by analyzing the distributions of velocity (Fig. 2) and temperature (Fig. 3) on the plane (axis) of symmetry. The coordinate $\bar{s} = s/R$ in Figs. 2 and 3 is counted from the front stagnation point in the upstream direction.

It follows from Fig. 2 that a normal shock wave is formed ahead of the body at the initial time; the shock wave is located closer to the body and the change in velocity in this shock wave is greater than that in the case of the normal shock wave in an inviscid gas (relative flow velocity behind the normal shock is $u_1/V_\infty = 0.2$ for $M_\infty = 5$ and the ratio of specific heats $\gamma = 1.4$). At subsequent times, the shock wave moves upstream, and the ratio u_1/V_∞ approaches the value for the inviscid gas. The flow velocity between the shock wave and the body changes linearly.

The distribution of the pressure coefficient ahead of the body on the plane (axis) of symmetry has a similar character. At the initial time, flow deceleration in the shock wave in the viscous gas proceeds with lower total pressure losses, as compared to the inviscid gas. For instance, for $\bar{t} \leq 1$, the pressure coefficient at the stagnation point on the cylinder is $c_p \geq 2$, whereas the corresponding value for the inviscid steady flow is $c_p = 1.75$. At later times, the total pressure losses in the shock wave increase, and the viscous solution approaches the inviscid solution from above.

It is of interest to consider the temperature distributions on the plane (axis) of symmetry ahead of the body (Fig. 3). At the beginning of flow development, the gas temperature in the region between the shock wave and the body is significantly higher than the free-stream stagnation temperature ($\bar{T}^* = T^*/T_\infty = 6$). For example, at the time $\bar{t} = 1$, the maximum relative temperature in the region between the shock wave and the body is $\bar{T}_{\max} \approx 8$ for the cylinder and $\bar{T}_{\max} \approx 7$ for the sphere. Subsequently, the maximum temperature in this region decreases and approaches the free-stream stagnation temperature from above.

The position of the local maximum in temperature distributions corresponds to the external boundary of the thermal boundary layer. It follows from the data in Fig. 3 that the inviscid and viscous flows are developed simultaneously and interact.

Flow on the Plane (Axis) of Symmetry behind the Body. Let us analyze the distributions of gas-dynamic variables on the plane (axis) of symmetry behind the bodies considered. According to data in Fig. 4, where the coordinate $\bar{s} = s/R$ is counted from the rear stagnation point in the downstream direction, the flow can be divided into three regions: viscous flow, transitional (quasi-inviscid) flow, and undisturbed uniform flow. At the initial stage of evolution, the gas flow in the base region is attached, and a viscous region of the disturbed flow with a linear velocity profile ($\bar{t} = 1$) is formed between the body and the departing front of the disturbed flow. At later times, the longitudinal size of the disturbed flow increases, and a global separated flow region originates and

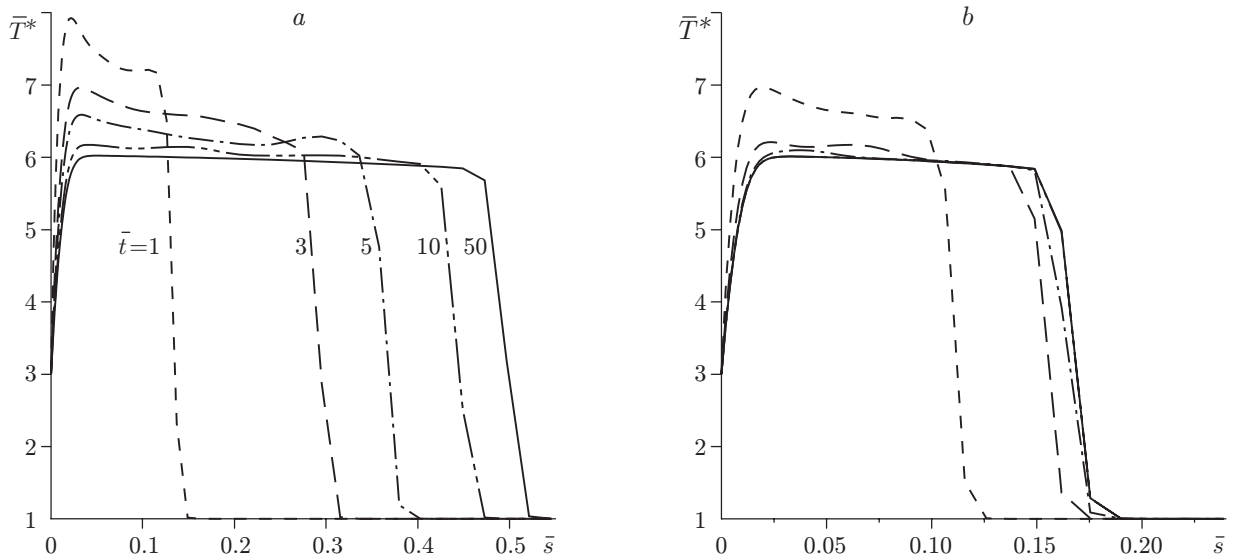


Fig. 3. Distribution of the stagnation temperature $\bar{T}^* = T^*/T_\infty$ on the axis of symmetry ahead of an isothermal cylinder (a) and an isothermal sphere (b) at different times.

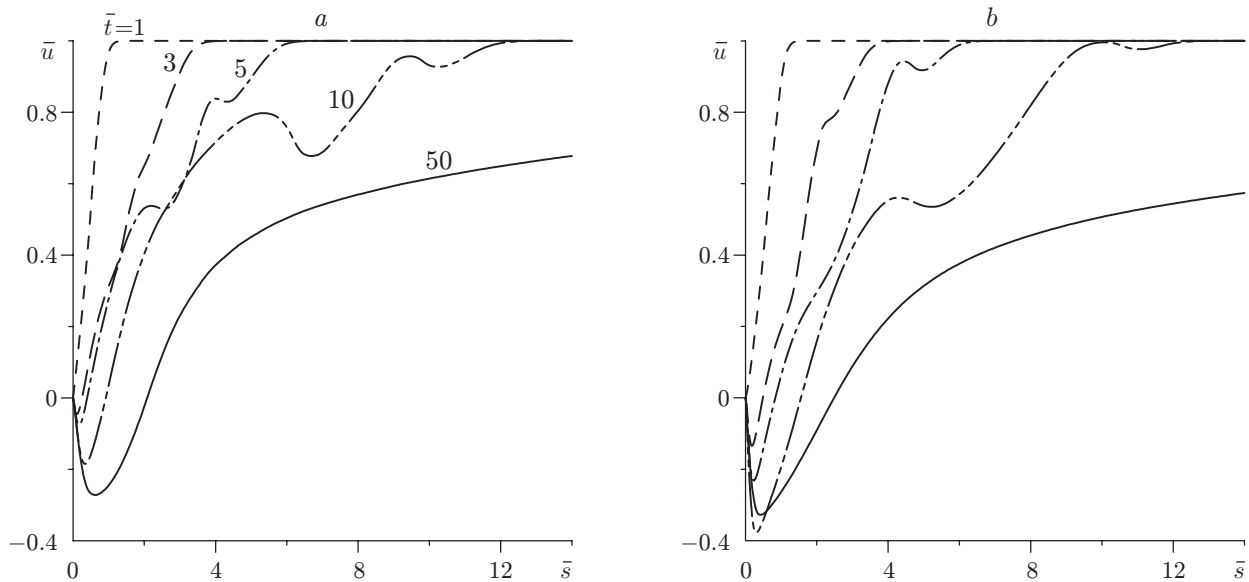


Fig. 4. Distribution of velocity $\bar{u} = u/V_\infty$ on the axis of symmetry behind an isothermal cylinder (a) and an isothermal sphere (b) at different times.

develops in the neighborhood of the rear stagnation point ($\bar{t} = 3$); a transitional zone is formed in the neighborhood of the departing front. In what follows, further development of the global separated flow region occurs, the size of the transitional zone increases, and compression and rarefaction waves appear there. At $\bar{t} \geq 10$, the free-stream front almost leaves the computational domain, and the transitional zone, which has a complex structure, is located in the neighborhood of the output boundary of the computational domain. By this time, the near wake structure has been already formed. At later times, the transitional zone leaves the computational domain, and the near wake structure transforming to the far wake structure is developed ($\bar{t} = 50$). Note, the value of the derivative $\partial u/\partial s$ at the rear stagnation point remains almost unchanged after the moment the global separation region appears.

The pressure coefficient in the flow region behind the body (in contrast to the flow region ahead of the body) changes insignificantly as a whole. At the initial time, noticeable rarefaction arises in the neighborhood of the rear stagnation point, which decreases later but remains finite until the steady state is reached. The pressure coefficient in the longitudinal direction changes monotonically until global separation incipience. At subsequent times, the monotonic character of the dependence $c_p(\bar{s})$ is violated.

It follows from the analysis of temperature distributions that the uniform low-temperature supersonic flow in the region behind the body is gradually displaced by a high-temperature vortex gas flow. In the course of evolution, the gas temperature in the region considered is lower than the stagnation temperature of the supersonic free stream.

Conclusions. An analysis of the evolution of the flow field and aerodynamic characteristics of a circular cylinder and sphere instantaneously starting with a constant supersonic velocity ($M_\infty = 5$ and $Re = 10^5$) from the state at rest revealed some interesting features.

In contrast to an incompressible liquid, inviscid and viscous flows in a gas are simultaneously developed and interact. Therefore, because of unsteady and viscous effects, flow deceleration in the shock layer ahead of the body in the beginning of flow evolution occurs with lower total pressure losses than in the case of an inviscid normal shock wave, and the maximum gas temperature behind the shock wave is higher than the free-stream stagnation temperature. With time, the solution of the problem asymptotically approaches the solution for the normal shock wave.

An attached flow around the body is formed in the near wake in the initial period. Complicated reconstruction of the flow field occurs at the moment of global separation incipience. Then, a closed zone of global separation and the structure of the near and far wake typical of a steady flow around the bodies considered is gradually formed.

REFERENCES

1. L. G. Loitsyanskii, *Mechanics of Liquids and Gases*, Pergamon Press, Oxford–New York (1966).
2. G. Schlichting, *Boundary Layer Theory*, McGraw-Hill, New York (1968).
3. V. A. Bashkin, I. V. Egorov, and M. V. Egorova, “Supersonic perfect-gas flow around a circular cylinder,” *Izv. Ross. Akad. Nauk, Mekh. Zhidk. Gaza*, No. 6, 107–115 (1993).
4. V. A. Bashkin, I. V. Egorov, and D. V. Ivanov, “Application of the Newton method to the calculation of internal supersonic separated flows,” *J. Appl. Mech. Tech. Phys.*, **38**, No. 1, 26–37 (1997).